Challenges for the interconnection of crystalline silicon heterojunction solar cells

Angela De Rose, Torsten Geipel, Denis Erath, Achim Kraft & Ulrich Eitner, Fraunhofer Institute for Solar Energy Systems ISE, Freiburg, Germany

Abstract

Crystalline silicon heterojunction (HJT) solar cells and modules based on amorphous silicon on monocrystalline wafers offer advantages over established wafer-based technologies in terms of efficiency potential, complexity of the manufacturing process, and energy yield of the modules. The temperature sensitivity of these solar cells, however, poses considerable challenges for their integration in modules. Currently, there exist three approaches for the interconnection of HJT solar cells, each with its own strengths and weaknesses: 1) ribbon soldering with low-melting-point alloys; 2) gluing of ribbons by using electrically conductive adhesives (ECAs); 3) SmartWire Connection Technology (SWCT). This paper provides an overview of the different approaches and focuses on ribbon-based interconnection technologies. Soldering at process temperatures below 200°C enables standard stringing equipment to be used, but this method is known to result in weak adhesion of the low-temperature metallization pastes on the cell surface. This study focuses on the microstructure of the solder joints for such pastes, and an indication of the origin of the associated low peel strength is given. The dependence of the quality of ECA-based interconnections on curing conditions is analysed with regard to printability, electrical properties and peel strength. Recent results for different ECAs processed using a mass-production stringer are presented, and a 60-cell HJT module exceeding 320Wp is demonstrated.

Silicon heterojunction cell technology

There is a growing interest in semiconducting hetero-structures in PV fabrication lines for silicon solar cells. Within the last few years, several impressive photoconversion efficiencies for heterojunction (HJT) solar cells on n-type wafers have been reported. The highest efficiencies have been achieved in combination with an interdigitated back-contact (IBC) design, as in 2017 by Kaneka with 26.7% (designated area, da: 79cm^2) and 26.3% (da: 180.4cm^2) [1,2], or in 2014 by Panasonic with 25.6% (da: 143.7cm^2) [3]. For two-side-contacted HJT cells, Kaneka achieved 25.1% (aperture area: 151.9cm^2) in 2015 [4], and Panasonic showed 24.7% with a wafer thickness <100µm (total area: 101.8cm^2) in 2014 [5].

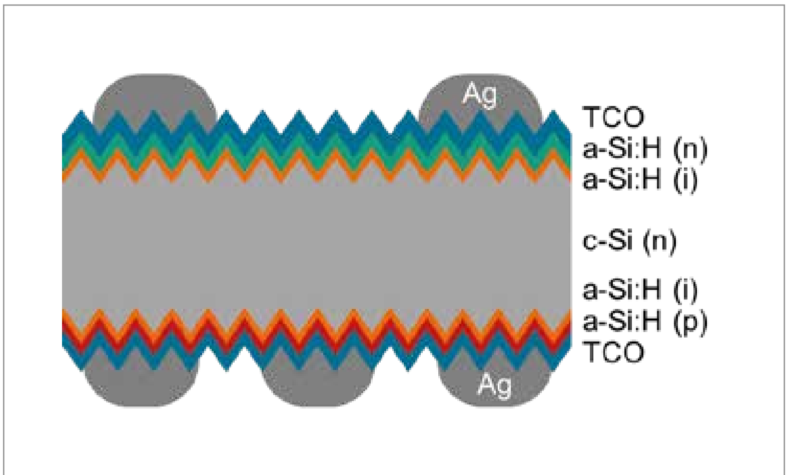

Figure 1. Schematic of a bifacial silicon HJT solar cell with an n-type c-Si wafer, rear emitter and a-Si:H layer for excellent passivation. (Not drawn to scale.)

A major advantage of HJT solar cells over homojunction cells is the optimized quality of the interface between the c-Si wafer and the a-Si layer; this enables a high passivation quality and leads to the suppression of recombination at the surface of the wafer, and therefore to a higher open-circuit voltage (730–750mV). Additionally, thinner Si wafers (<165µm), the high quality of the deposited amorphous thin film layers and the improved fill factor (>82%) allow one to get close to the theoretical conversion efficiency limit of Si solar cells. The HJT technology facilitates a lower temperature coefficient of power, enabling superior module performance compared with homojunction cells [2,6]. One of the possible structures of an HJT solar cell that requires an interconnection of both sides is shown in Fig. 1.

Besides the high performance of HJT solar cells, the corresponding production chain is fairly lean, consisting of low-temperature (<200°C) processes [7]. The deposition of the hydrogenated amorphous silicon (a-Si:H) is usually implemented by plasma-enhanced chemical vapour deposition (PECVD). The transparent conductive oxide (TCO) layers, typically indium tin oxide, are deposited by sputtering, whereas the metal contacts on the front side are currently fabricated by screen printing of silver-containing pastes or electroplating of copper [2,8].

Screen-printed metallization for HJT solar cells

Owing to the temperature sensitivity of the a-Si:H layers [9], low-temperature screen-printing pastes are used as the metal grid electrode on top of the TCO layer. Being a conductive metal, silver is widely used; a promising alternative, however, is copper, which takes advantage of the low process temperatures. Similarly to conductive adhesives, low-temperature metallization pastes mainly consist of a polymer (or more than one polymer) and a conductive metal in the form of particles or flakes. The thermal treatment after printing, typically performed at a temperature ≤200°C, forces the solvents to evaporate from the paste.

> "Since the polymer remains in the low-temperature metallization paste after curing, guaranteeing low resistivity is a challenge."

Most commonly, thermo-setting pastes are used, where the polymers cross-link and form a matrix in which the conductive metal is stabilized during the curing process. Thus, in contrast to high-temperature metallization pastes with sintering temperatures above 700°C, the polymer is not thermally removed from the resulting metallization; furthermore, the polymer determines the adhesion and conductivity properties of the paste after curing. Since the polymer remains in the low-temperature metallization paste after curing, guaranteeing low resistivity is a challenge. Typically, the line resistivity is a factor of two to three times higher (typically 5–8μΩcm) than that for sintered high-temperature silver pastes. In contrast, the contact resistivity of the metallization on the TCO can be as low as that for high-temperature process schemes (<4mΩcm^2) [10].

The paste composition is highly affected by the cell interconnection concept (discussed later) and the curing process used; this means that there will need to be a trade-off between the required conductivity, fine-line printability and adhesion properties of the wafer surface and the ribbon for interconnection. For a metallization approach with busbars, printing processes for busbars and fingers can be split into two single process steps, allowing separate paste optimizations. A cured busbar of an HJT solar cell is shown in the scanning electron microscopy (SEM) image in Fig. 2.

In the last couple of years, the processability and fine-line printability of low-temperature pastes have improved remarkably, already allowing screen openings for the contact fingers down to 40μm in an industrial production environment. On a laboratory scale, a printed line width of <35μm with a screen opening of 30μm and below has been demonstrated with a reliable single screen-printing process [10].

Another aspect of paste development focuses on the reduction of the curing time. To date, a curing duration of up to 30 min is typically employed in order to achieve sufficient conductivity and adhesion. To allow high throughput in an industrial environment, cassette furnaces are widely used; here, the wafers are sorted into heat-stable carriers, which are then transported through the oven. As an alternative, inline furnaces with multiple wafer tracks on ceramic rollers or on a mesh belt can be used; however, these furnaces are often space-consuming because of the length of the process chamber required to provide high throughput.

Interconnection technologies for HJT solar cells

Besides the choice of materials for module integration, the interconnection of HJT cells is still challenging and research is ongoing. The most widely known approaches are briefly presented below, with the focus being on the busbar-based low-temperature interconnection by soldering and gluing.

Low-temperature soldering

Busbar interconnection

For the interconnection of HJT solar cells, the cheapest and most straightforward implementation into existing fabrication lines is soldering at lower temperatures; this allows the use of standard stringing equipment for ribbon soldering on automated stringers. Solder-coated Cu ribbons are aligned on both sides of the cell to contact the Ag busbar and to electrically connect several cells in series. To satisfy the requirement of lower process temperatures for HJT solar cells, bismuth (Bi)-based solders serve as an alternative to lead-containing solder alloys. Details and current challenges for low-temperature soldering on the low-temperature metallization of HJT solar cells will be presented in a later section.

SmartWire Connection Technology

As an alternative to conventional busbar-based interconnection processes, Meyer Burger Technology AG commercializes SmartWire Connection Technology (SWCT) [11,12]: this approach combines lamination with interconnection using thin round Cu wires coated with a low-temperature solder. For accurate positioning, the wires are embedded into an additional polymer foil before lamination. A 335Wp module with 60 cells and an average cell efficiency of 23.5% has been reported [13].

ECAs

An option for realizing a ribbon-based interconnection with low thermomechanical stress that is suitable for HJT solar cells is the use of ECAs [14]; this approach is commercialized by the company teamtechnik [15]. ECAs basically consist of a polymeric adhesive, such as an epoxy, acrylate or a silicone, filled with electrically conductive particles. The filler content is usually above the percolation threshold, which is 25–30%$_{vol.}$ for typical adhesives [16]. ECAs are applied by screen printing or other methods. After the material application, the ribbons are positioned and the ECA is thermally cured; the curing leads to cross-linking of the polymer chains

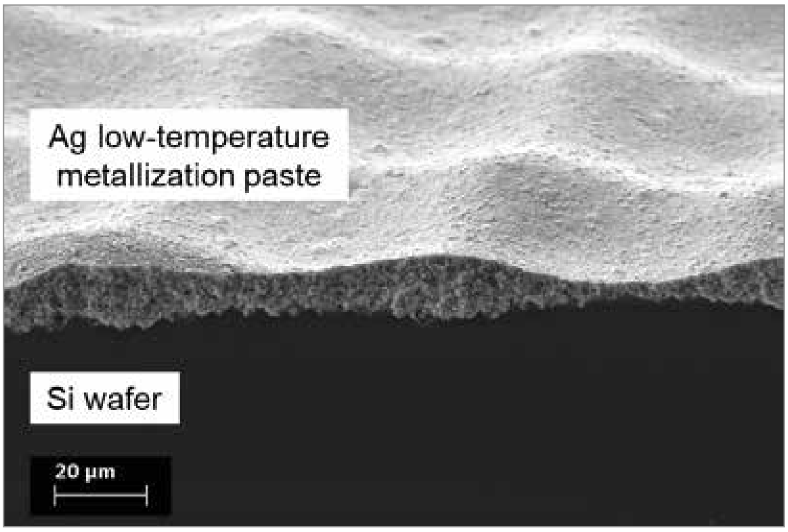

Figure 2. SEM cross-section image of low-temperature screen-printing paste after curing for the metallization of HJT solar cells.

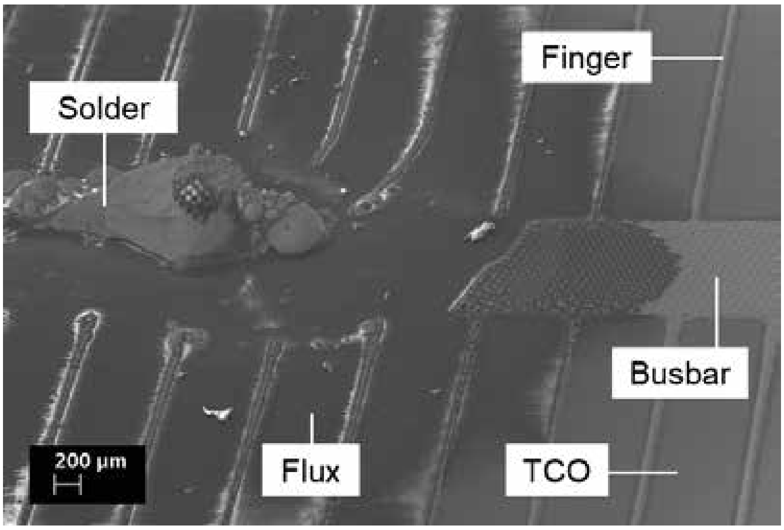

Figure 3. Top-view SEM image taken from a wetting test with liquid solder on a low-temperature metallization paste. The paste is breaking away from the cell surface directly after contact with the solder.

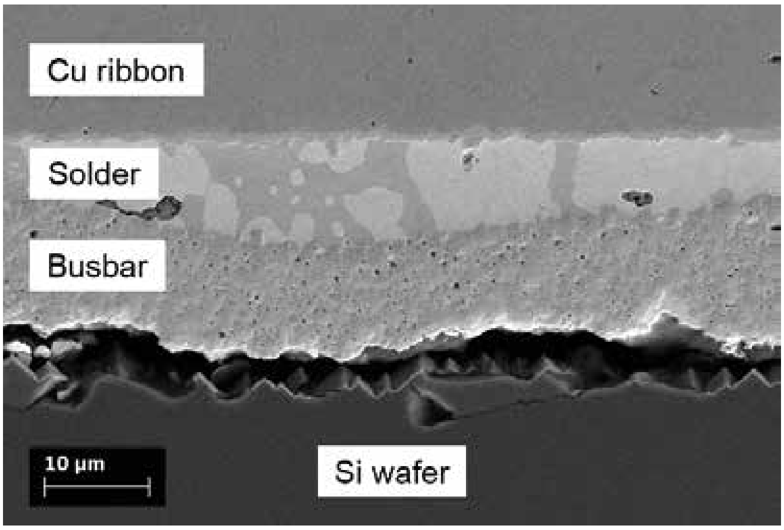

Figure 4. SEM image of the cross section of an HJT solar cell after soldering. Wetting of the busbar by liquid SnBi solder is conceivable, but the adhesion of the paste to the wafer is insufficient.

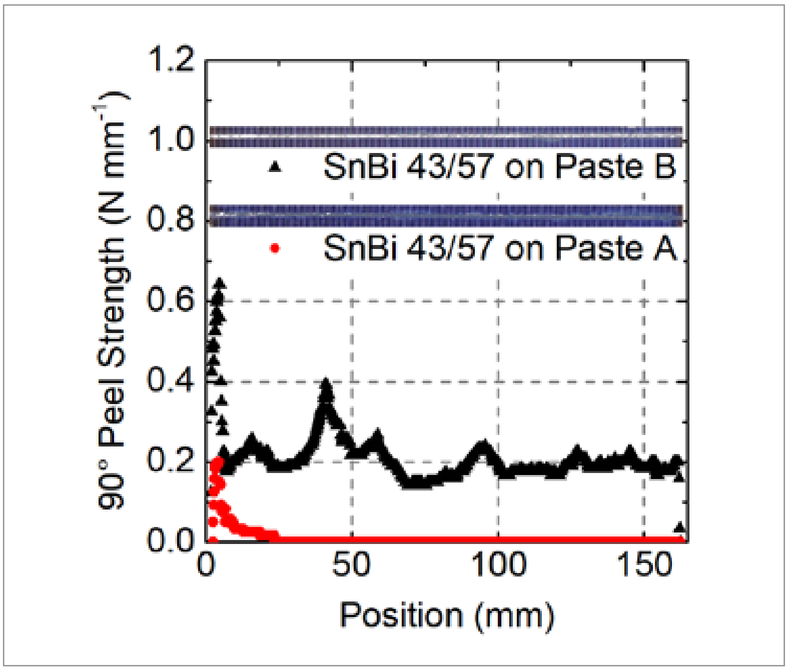

Figure 5. Results of a 90° peel test for SnBi-coated Cu ribbons soldered onto different low-temperature metallization pastes on an HJT solar cell. Corresponding fracture patterns (top-view images of the busbar after the peel test) are shown at the top. (Adapted from De Rose et al. [17].)

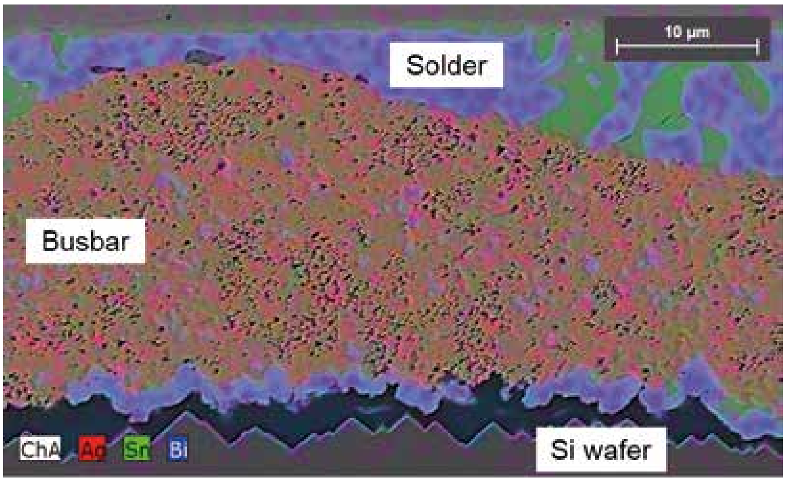

Figure 6. EDX mapping of a solder joint on an HJT low-temperature metallization paste. Diffusion of the solder (Sn, Bi) into the busbar (Ag) reduces the adhesion at the Si wafer. (Adapted from De Rose et al. [17].)

Figure 7. The TT1600 ECA solar cell stringer from the Germany-based company teamtechnik, capable of producing glued HJT strings at a throughput of 2.3 sec per cell and 1,600 cells per hour.

"The major challenge for the busbar interconnection of HJT solar cells is the metallization paste adhesion to the wafer surface."

and to adhesion to the surfaces. The challenges for the interconnection of HJT solar cells with ECAs will be addressed in detail in a later section.

Challenges for busbar-based soldering technology

The temperature sensitivity of the a-Si layers on HJT solar cells, and the trend towards thinner Si wafers [5], limit the applicable processes and materials for interconnection. Since the a-Si passivation will not withstand temperatures above 250°C [7,9], solder alloys with a lower melting point than eutectic SnPb solder (T_{liq} ≈ 180°C, $T_{process}$ ≈ 250°C) have to be employed. Bi-based alloys have melting points between 120°C and 160°C and can be soldered at process temperatures below 200°C; moreover, they provide a lead-free alternative for compliance with the future restriction of hazardous substances (RoHS) requirements for solar modules.

Tape and shear tests on low-temperature pastes reveal that the adhesion before soldering is lower than that for standard Ag firing pastes [17,18]. The soldering process will usually reduce the initial adhesion on HJT metallization. When the molten solder comes into contact with the paste, it fully wets the busbar and, in most cases, quickly decomposes the metallization (see Fig. 3). After soldering a busbar with a SnBi-coated ribbon, the paste tends to detach from the wafer surface, which is illustrated in the SEM cross-section image in Fig. 4. The interaction with the solder is specific to each individual metallization, driven by different compositions of the low-temperature pastes.

In contrast to solder joints on high-temperature silver pastes, an evaluation with a 90° peel test in accordance with DIN EN 50461 reveals a peel strength below the required limit of 1Nmm^{-1} [19]. An example with two commercially available low-temperature pastes is given in Fig. 5. In this soldering example, the corresponding fracture patterns reveal an adhesive fracture with zero adhesion (paste A), and a mostly cohesive fracture within the paste with an average peel strength of around 0.2Nmm^{-1} (paste B).

It was found that the liquid solder penetrates the metallization during the soldering process, as detected by electron diffractive X-ray (EDX) spectroscopy (Fig. 6) [17]. Sn diffuses homogeneously, whereas Bi clusters and agglomerates at the interface with the wafer; this behaviour is highly dependent on the grain structure of the metallization paste. The formation of the Bi layer supports ablation of the paste, since Bi has a negative coefficient of thermal expansion and expands when it solidifies [20]. Other researchers assume that the temperature shock during soldering leads to a weaker interface between the paste and the cell [18]. Additionally, the coefficient of thermal expansion (CTE) mismatch between copper and the silicon wafer adds thermomechanical stress.

The major challenge for the busbar interconnection of HJT solar cells is the metallization paste adhesion to the wafer surface. On the way to creating a successful solar cell interconnection, the soldering parameters need to be carefully adjusted, and an adaptation of the low-temperature metallization pastes is essential. Besides an optimization of the conductivity and printability, the adhesion to the wafer has to be addressed and the diffusion of liquid solder prevented.

Challenges for ECA technology

A fully-automated stringer capable of the industrial interconnection of HJT solar cells either by low-temperature soldering or by gluing of ECAs is available at Fraunhofer ISE in Freiburg, Germany – the TT1600 ECA stringer is provided by the Germany-based company teamtechnik GmbH (see Fig. 7) [15]. With a throughput of 2.3 sec per cell with today's ECA cure durations, the stringer enables a production of 1,600 cells per hour. The stringer utilizes screen printing as an application method for ECAs, and is equipped with infrared lamps and heating plates to realize a fast and efficient curing process [21].

Conductive adhesives as a lead-free and compliant interconnection technology have been investigated by many groups over the last few years [22–27]. Recently, an increasing interest shown by the industry in this technology has been observed [28]. Within the joint research project KleVer (BMWi Contract No. 03258338), teamtechnik and Fraunhofer ISE assessed numerous commercially available ECAs in terms of printability, electrical properties, peel strength and cure speed, and module performance with the goal of improving ECA technology.

Printability

The printability of ECAs with the screen-printing unit in the stringer is evaluated in terms of pot life, print uniformity and lay-down (the amount of printed ECA). The *pot life* is the time period in which the mixed and thawed-out ECA (after having been stored in a frozen state) is processable without impairment of the printing or other important

"Thanks to recent developments in ECA chemistry, many materials today achieve a peel strength of more than 0.5Nmm^{-1}."

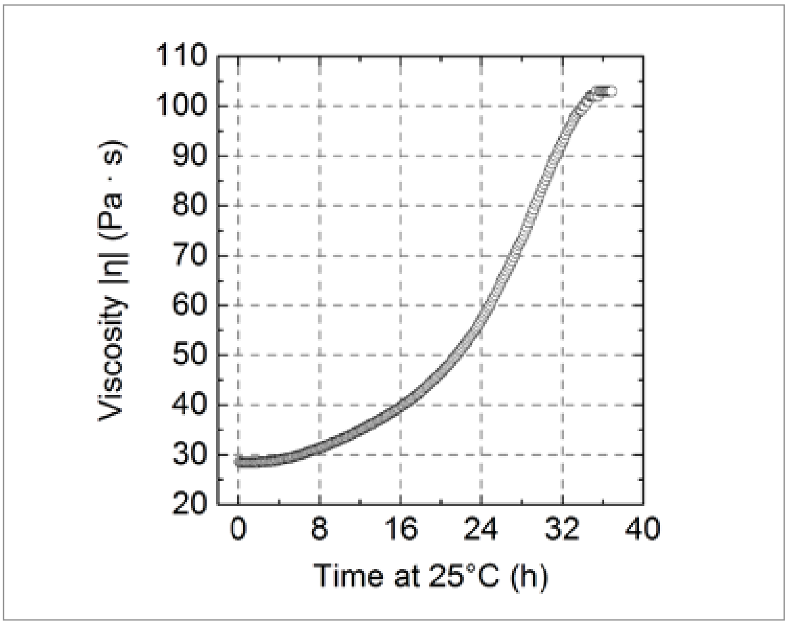

Figure 8. Dependency of the viscosity of a tested ECA on the exposure time at 25°C (measured with a plate–plate rheometer at a constant shear rate of 10s^{-1}).

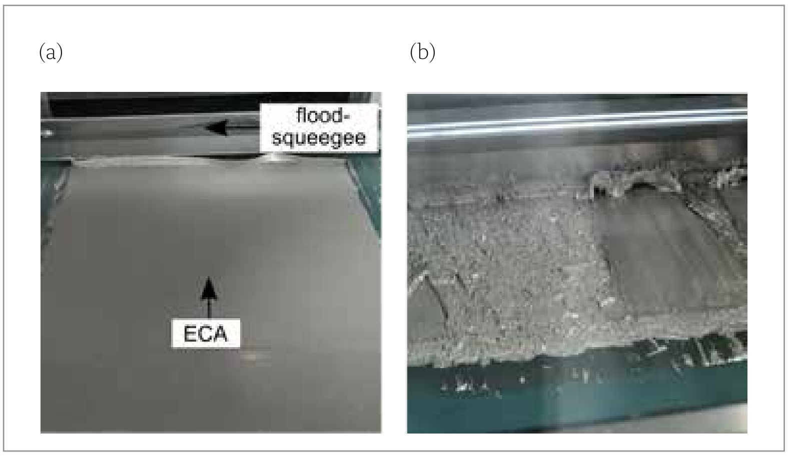

Figure 9. (a) Uniform flooding of the screen with ECA. (b) Non-uniform flooding of an ECA with a viscosity that is too high.

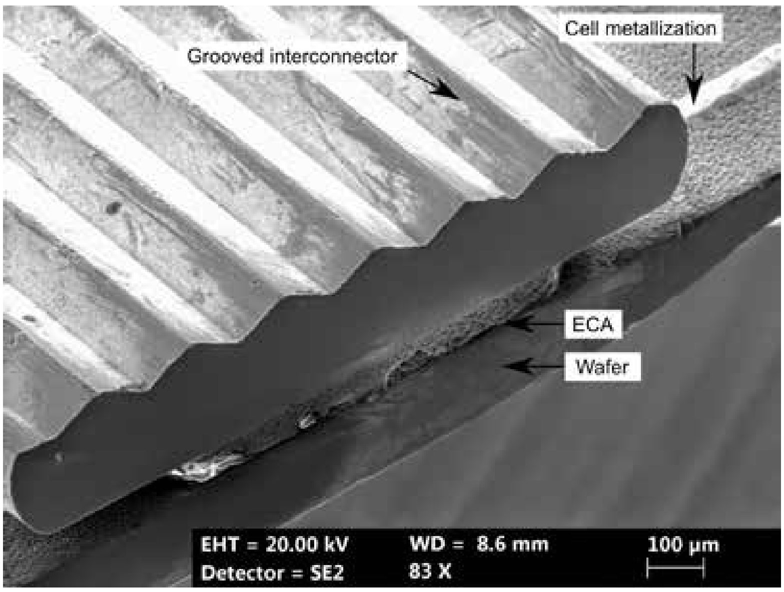

Figure 10. SEM image of a grooved interconnector glued directly to the finger metallization of a solar cell.

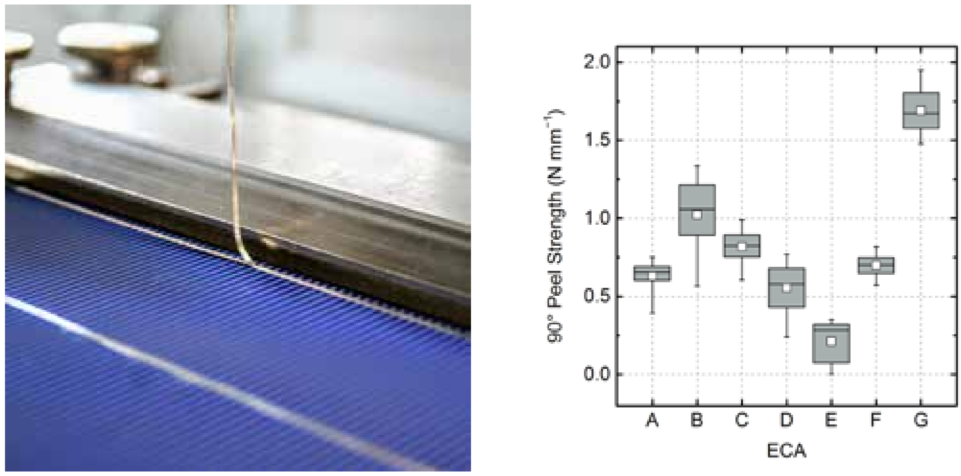

Figure 11. Peel test and peel strength data for ECAs. (Box = 25–75 percentiles; white square = mean; horizontal line = median; whisker = 5–95 percentiles.)

properties. It is limited by the reactivity of the glue components at ambient temperature and should exceed eight hours (i.e. one production shift).

The pot life can be determined by rheological measurements, as shown in Fig. 8. In this example, the tested adhesive has an initial viscosity of approximately 30Pa·s at a shear rate of $10s^{-1}$; after eight hours at ambient temperature, the viscosity barely changes. In conclusion, the printability does not change very much in eight hours (see Fig. 9(a)). After 24 hours, however, the viscosity doubles, which could potentially give an undesirable printing result. In particular, very fast curing adhesives may suffer from reduced pot life. A fast cure is required for high throughput, but an overly high viscosity leads to non-uniform screen flooding as shown in Fig. 9(b), and to clogged screens and a lack of applied adhesive in a worst-case scenario.

The amount of printed ECA currently ranges from 6mg to 15mg per busbar and is highly dependent on the filler content of the adhesive, viscosity and screen configuration. With an optimized bond design there is room for further reduction in consumption.

An SEM image of a fully printed and cured ECA interconnection with the use of grooved interconnectors directly on the solar cell metallization is shown in Fig. 10. The grooved interconnectors consist of a Cu core and a thin (<1μm) Ag coating that protects the copper from oxidation. The grooved structure of the ribbon improves the short-circuit current of the module by 2–3% compared with conventional flat ribbons [29].

Electrical properties

The electrical properties of ECA interconnections are determined by the volume resistivity of the ECA and the contact resistivity at the bonded surfaces.

The volume resistivity is measured in accordance with the method specified in MIL-STD-883H (section 5011.5) [30], and often ranges between 10^{-4} and $10^{-3}\Omega$cm for many commercially available ECAs. This value is sufficiently low as to not reduce the fill factor of the PV module [31,32]. A correlation exists between volume resistivity and cure temperature: usually, increasing the cure temperature leads to stronger material shrinkage and a more efficient lubricant removal around the filler particles, and thus to a significant decrease in volume resistivity [33,34].

The contact resistivity of ECAs on silver surfaces is as low as that of a soldered bond, and lies within the range 10^{-3}–10^{-2}mΩcm^2 [26]. In the case of non-noble metal surfaces, however, the contact resistivity can be noticeably higher under initial conditions, and may further degrade if ageing takes place [35,36]. Nevertheless, stabilizing the contact resistivity on non-noble metals has the potential for further cost reductions, since the Ag coating around the ribbon could be replaced.

Threshold values for volume and contact resistivity are proposed in the authors' recent publication [31].

Peel strength and cure speed

Low peel strength is often regarded as a significant drawback of ECA technology, despite the demonstration of reliability in thermal cycling tests [37]. The reasons for the limitation in peel strength are partly synonymous with the above-mentioned difficulties of low-temperature metallization pastes. A liquid metal diffusion – relevant to low-temperature paste soldering – does not play a role in ECA interconnection strength; however, ECAs and low-temperature pastes are both based on filled polymers, which lack toughness compared with metals.

Thanks to recent developments in ECA chemistry, many materials today achieve a peel strength of more than 0.5Nmm^{-1}, sometimes even surpassing 1Nmm^{-1}; this is usually sufficient for handling the strings and for withstanding thermal cycling tests. Summarized peel strength data for ECAs glued onto HJT cells are shown in Fig. 11. The fracture mode for the tested ECAs is *cohesive*, indicating proper adhesion to the surfaces. Since higher peel strength is achieved by increasing the ECA lay-down, there is a trade-off with material consumption and costs, which has to be determined.

An improper cure is often the cause of inadequate peel strength. Fig. 12 shows the peel strength of adhesive A as a function of cure temperature and time. The default curing schedule of adhesive A is 30 sec at a constant temperature of 180 to

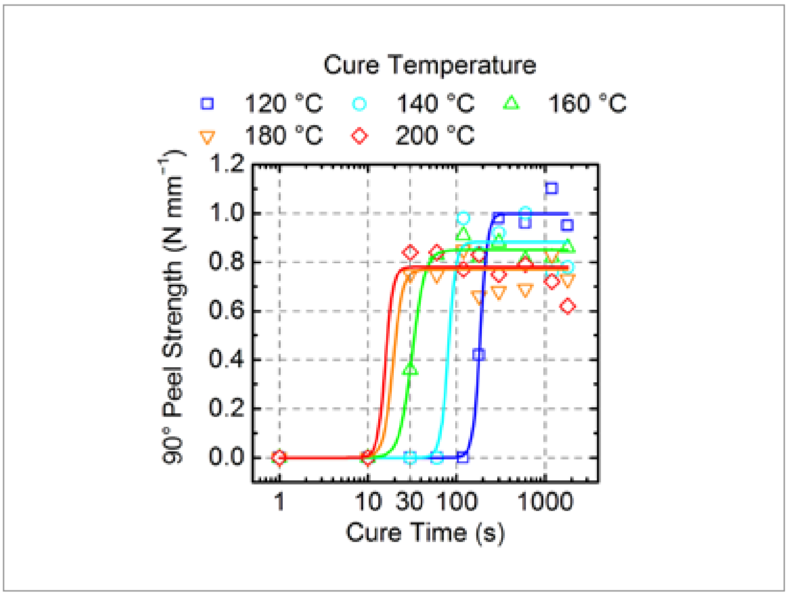

Figure 12. Dependence of the peel strength of adhesive A on the curing temperature and time. Each symbol is the average of several peel tests. (The interpolated solid lines are simply a guide.)

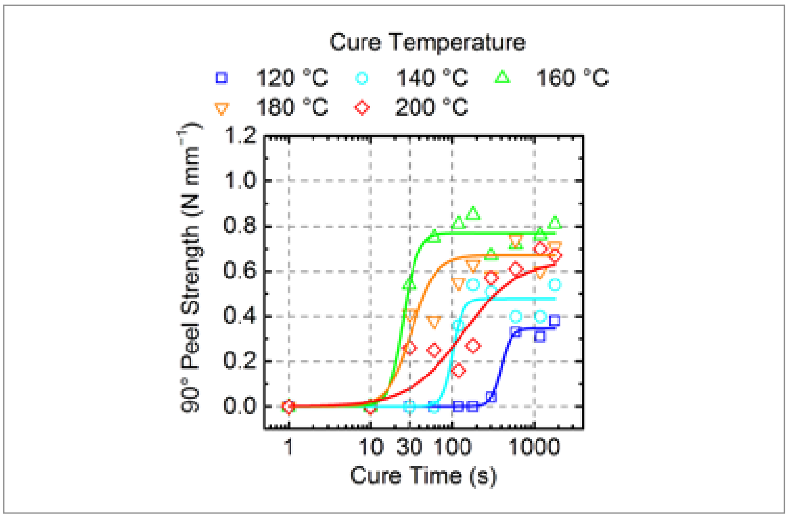

Figure 13. Dependence of the peel strength of adhesive B on the curing temperature and time. Each symbol is the average of several peel tests. (The interpolated solid lines are simply a guide.)

"A 320Wp module based on glued HJT solar cells was demonstrated to yield significantly more power than state-of-the-art PERC modules."

Figure 14. 320Wp HJT module, as produced in the Module-TEC laboratory at Fraunhofer ISE.

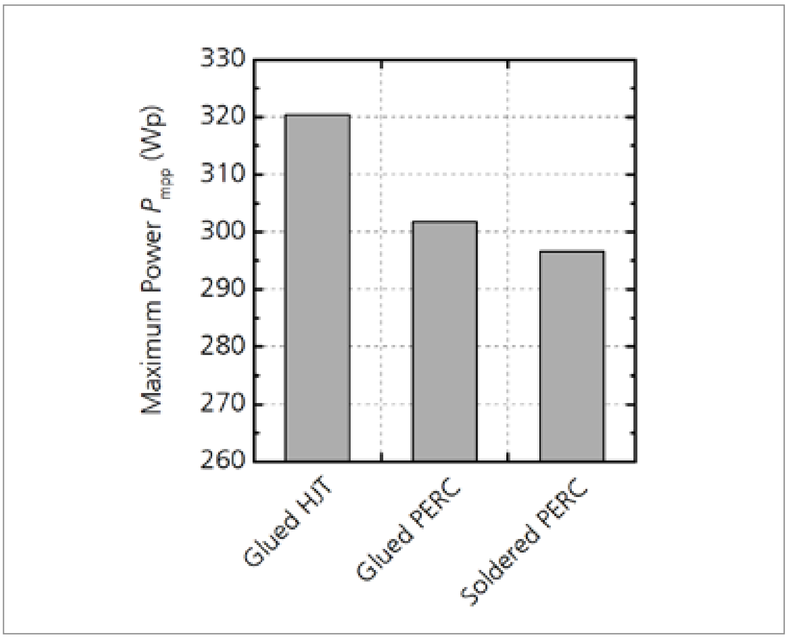

Figure 15. Power comparison of HJT modules and PERC modules.

200°C. With this schedule, adhesive A obtains its maximum peel strength of 0.8–1.0Nmm^{-1} and remains at this level, even after curing for a very long duration (e.g. in the case of a machine stoppage). The peel strength does not significantly decrease if the bond is exposed to prolonged heating – one of the differences from busbar soldering. A cure temperature of 160°C results in a cure duration of 60 sec before the adhesive achieves its full peel strength; for temperatures below 160°C, however, the adhesive requires several minutes to cure. Usually, a curing temperature that is too low results not only in unreasonably high cure durations but also in increased volume resistivity.

Fig. 13 depicts the peel strength of adhesive B as a function of time and temperature: a maximum peel strength is achieved after curing for 60 sec at 160°C. For temperatures above 160°C, the peel strength is reduced and is recovered only by prolonging the cure duration. In the case of adhesive B, a temperature below 140°C will not cure the adhesive at all, even after an extended cure time; this is because the activation of the curing agent in the adhesive chemistry is obstructed.

For chemistries such as adhesive A, it is sufficient to use a constant, relatively high temperature (180–200°C) to cure the material in the stringer. Other adhesives require an adjusted cure profile with soft ramp-up and cool-down phases, which needs to be tested case by case in production trials. Fraunhofer ISE has developed specific software to simulate the cure of ECAs and other polymers for complex temperature profiles [38].

Module performance

The module integration of HJT cell strings requires the appropriate choice of encapsulation materials in order to obtain a module yielding high performance and reliability. Recently, a module power of 320Wp with 60 cells was demonstrated by Fraunhofer ISE [21]; this module was produced in the Module-TEC laboratory and is depicted in Fig. 14. The current–voltage characteristic is marked by a high short-circuit current of 9.3A, thanks to the grooved interconnectors and AR-coated glass. Furthermore, the fill factor is high, with a value of 78.1%, as a result of an optimized finger design at the cell level, a good choice of ECA and the reliable processing of the teamtechnik stringer.

The use of heterojunction technology in combination with an ECA-based interconnection process leads to a boost in module performance by just over 20Wp compared with a state-of-the-art passivated emitter and rear cell (PERC) and conventional solder technology, as can be seen in Fig. 15.

Conclusion

Silicon heterojunction technology has the potential for further improvements in efficiency over PERC technology. However, the temperature sensitivity of the cell structure and, in particular, the low-temperature metallization pose new challenges for module integration. Besides a wire-based method with low-melting-point solders, there are options to use ribbon-based soldering with SnBi alloys or conductive gluing.

Low-temperature soldering with SnBi alloys is the most straightforward approach for the interconnection of HJT solar cells. According to Fraunhofer ISE's current research, the main challenge is the adhesion of the low-temperature metallization paste to the wafer surface. Because of the diffusion of liquid solder into the metallization, the peel strength of the interconnections is often critical for module integration. Further paste development with regard to grain structure, adhesion properties and microstructure may solve this problem, and thus enable a successful busbar interconnection with low-temperature solder alloys.

Low-temperature and lead-free RoHS-compliant ECA technology has significantly matured over the past few years thanks to the availability of high-throughput equipment for gluing, and because of the constant progress of adhesive manufacturers in improving printability, cure speed and peel strength and in driving down material costs. The TT1600ECA stringer at Fraunhofer ISE allows an analysis of ECAs in terms of their processability and readiness for mass production. Results regarding the challenge to preserve good printability at room temperature in combination with fast curing in the stringer have been presented. In addition, the complexity involved in finding the right cure profile for specific ECAs was highlighted. A peel strength of >1Nmm^{-1} was frequently measured during the testing. Finally, a 320Wp module based on glued HJT solar cells was demonstrated to yield significantly more power than state-of-the-art PERC modules.

References

[1] Green, M.A. 2017, "Solar cell efficiency tables (version 50)", *Prog. Photovolt: Res. Appl.,* Vol. 25, No. 7, pp. 668–676.
[2] Yoshikawa, K. et al. 2017, "Silicon heterojunction solar cell with interdigitated back contacts for a photoconversion efficiency over 26%", *Nat. Energy*, Vol. 2, No. 5, 17032.
[3] Masuko, K. et al. 2014, "Achievement of more than 25% conversion efficiency with crystalline silicon heterojunction solar cell", *IEEE J. Photovolt.*, Vol. 4, No. 6, pp. 1433–1435.
[4] Adachi, D., Hernández, J.L. & Yamamoto, K. 2015, "Impact of carrier recombination on fill factor for large area heterojunction crystalline silicon solar cell with 25.1% efficiency", *Appl. Phys. Lett.*, Vol. 107, No. 23, 233506.
[5] Taguchi, M. et al. 2014, "24.7% record efficiency HIT solar cell on thin silicon wafer", *IEEE J. Photovolt.*, Vol. 4, No. 1, pp. 96–99.
[6] De Wolf, S. et al. 2012, "High-efficiency silicon heterojunction solar cells: A review", *GREEN*, Vol. 2, No. 1, pp. 7–24.
[7] Korevaar, B.A. et al. 2008, "Influence of annealing on performance for hetero-junction a-Si/c-Si devices", *Proc. 23rd EU PVSEC*, Valencia, Spain.
[8] Rodofili, A. et al. 2017, "Laser transfer and firing of NiV seed layer for the metallization of silicon heterojunction solar cells by Cu-plating", *Solar RRL*, Vol. 114, DOI: 10.1002/solr.201700085.
[9] De Wolf, S. & Kondo, M. 2009, "Nature of doped a-Si: H/c-Si interface recombination", *J. Appl. Phys.*, Vol. 105, No. 10, 103707.
[10] Erath, D. et al. 2017, "Comparison of innovative metallization approaches for silicon heterojunction solar cells", *Energy Procedia,* Vol. 124, pp. 869–874.
[11] Soederstroem, T., Papet, P. & Ufheil, J. 2013, "Smart Wire Connection Technology", *Proc. 28th EU PVSEC*, Paris, France, pp. 495–499.
[12] Faes, A. et al. 2014, "SmartWire solar cell interconnection technology", *Proc. 29th EU PVSEC*, Amsterdam, The Netherlands, pp. 2555–2561.
[13] Meyer Burger 2017, "Meyer Burger Technology Day 2017 premiers heterojunction / SmartWire module with 335 watt efficiency as confirmed by TÜV Rheinland; Strong momentum in incoming orders confirmed", Press release (Nov. 30).
[14] Scherff, M.L.D. et al. 2006, "10 × 10 cm^2 HIT solar cells contacted with lead-free electrical conductive adhesives to solar cell interconnectors", *Proc. 4th WCPEC*, Waikoloa, Hawaii, USA, pp. 1384–1387.
[15] Teamtechnik GmbH 2018, "Innovative adhesive technology for industrial serial production: Stringer TT1400 ECA" [https://www.teamtechnik.com/en/solar/stringer-tt/stringer-tt1400-eca/].
[16] Lu, D.D. & Wong, C.P. 2009, "Electrically conductive adhesives (ECAs)", in *Materials for Advanced Packaging*, Lu, D.D. and Wong, C.P., Eds. New York: Springer US, pp. 365–405.
[17] De Rose, A. et al. 2017, "Low-temperature soldering for the interconnection of silicon heterojunction solar cells", *Proc. 33rd EU PVSEC*, Amsterdam, The Netherlands, pp. 710–714.
[18] Gierth, P. et al. 2013, "Comparison of NiV and polymer paste metallization as low temperature interconnection of high efficiency heterojunction solar cells", *Proc. 28th EU PVSEC*, Paris, France, pp. 464–467.
[19] DIN EN 50461 (2007-03), "Solar cells – Datasheet information and product data for crystalline silicon solar cells".
[20] Mei, Z. & Morris, J.W. 1992, "Characterization of eutectic Sn-Bi solder joints", *JEM*, Vol. 21, No. 6, pp. 599–607.
[21] Fraunhofer ISE 2018, "Fraunhofer ISE and teamtechnik demonstrate industrial maturity of electrically conductive adhesives for silicon solar cells", Press release (Apr. 25).
[22] Beier, B. et al. 2001, "Electrical conductive adhesives: A novel reliable method for interconnecting crystalline silicon solar cells", *Proc. 17th EU PVSEC*, Munich, Germany, pp. 812–815.
[23] Bennett, I. et al. 2007, "Low-stress interconnection of solar cells", *Proc. 22nd EU PVSEC*, Milan, Italy.
[24] Zemen, Y. et al. 2011, "Innovative and gentle interconnection technique for high efficiency c-Si solar cells and cost-of-ownership-analysis (COO)", *Proc. 26th EU PVSEC*, Hamburg, Germany, pp. 3125–3132.
[25] Schwertheim, S. et al. 2008, "Lead-free electrical conductive adhesives for solar cell interconnectors", *Proc. 33rd IEEE PVSC*, San Diego, California, USA, pp. 1–6.
[26] Geipel, T. & Eitner, U. 2013, "Electrically conductive adhesives: An emerging interconnection technology for high-efficiency solar modules", *Photovoltaics International*, 11th edn, No. 21, pp. 27–33.
[27] Schneider, A. et al. 2014, "Comprehensive study of material dependency for silver based conductive

glues", *Energy Procedia*, Vol. 55, pp. 509–518.
[28] Teamtechnik GmbH 2018, "Major contract for teamtechnik: Italian PV manufacturer orders stringers for production of high-efficiency modules with HJT cells", Press release (Feb. 12).
[29] Schneider, J. et al. 2014, "Combined effect of light harvesting strings, anti-reflective coating, thin glass, and high ultraviolet transmission encapsulant to reduce optical losses in solar modules", *Prog. Photovolt: Res. Appl.*, Vol. 22, No. 7, pp. 1–8.
[30] MIL-STD-883H: 2010-02, "Test method standard – Microcircuits.
[31] Geipel, T. et al. 2018 [forthcoming], "Optimization of electrically conductive adhesive bonds in photovoltaic modules", *IEEE J. Photovolt.*
[32] Hinz, I. et al. 2012, "Characterization of electrical conductive adhesives (ECA) for the photovoltaic-industry", *Proc. 27th EU PVSEC*, Frankfurt, Germany.
[33] Lu, D.D., Tong, Q.K. & Wong, C.P. 1999, "A study of lubricants on silver flakes for microelectronics conductive adhesives", *IEEE Trans. Compon. Packag. Technol.*, Vol. 22, No. 3, pp. 365–371.
[34] Lu, D.D. & Wong, C.P. 2000, "Effects of shrinkage on conductivity of isotropic conductive adhesives", *Int. J. Adhes. Adhes.*, Vol. 20, No. 3, pp. 189–193.
[35] Zwolinski, M. et al. 1996, "Electrically conductive adhesives for surface mount solder replacement", *IEEE Trans. Compon., Packag., Manuf. Technol. C*, Vol. 19, No. 4, pp. 241–250.
[36] Lu, D.D., Tong, Q.K. & Wong, C.P. 1999, "Mechanisms underlying the unstable contact resistance of conductive adhesives", *IEEE Trans. Electron. Packag. Manuf.*, Vol. 22, No. 3, pp. 228–232.
[37] Hoffmann, S. et al. 2017, "Analysis of peel and shear forces after temperature cycle tests for electrical conductive adhesives", *Proc. 33rd EU PVSEC*, Amsterdam, The Netherlands, pp. 183–186.
[38] Geipel, T. & Eitner, U. 2013, "Cure kinetics of electrically conductive adhesives for solar cell interconnection", *IEEE J. Photovolt.,* Vol. 3, No. 4, pp. 1208–1214.

About the authors

Angela De Rose studied physics at RWTH Aachen and at the University of Valencia, and received her master's in 2015 from RWTH Aachen. In 2016 she joined Fraunhofer ISE as a Ph.D. student in the field of interconnection technology for silicon PV modules. Her studies focus on the interconnection of HJT solar cells, soldering on aluminium surfaces and solder joint evaluation regarding long-term stability.

Torsten Geipel studied information system technology at the University of Dresden, Germany. He worked on 2D simulation of heterojunction solar cells at Helmholtz-Centre Berlin and received his Diploma degree in 2007. After spending four years in R&D with the former PV module manufacturer Solon, he began his Ph.D. thesis on electrically conductive adhesives at Fraunhofer ISE in the PV modules department. He recently completed his thesis and is currently working on cell interconnection and module integration.

Denis Erath studied printing technology at the University of Printing and Media in Stuttgart, Germany, and received his Diploma degree in 2005. Since then he has been with Fraunhofer ISE, working on various topics related to printing technologies for silicon solar cells and proton exchange membrane (PEM) fuel cells.

Dr. Achim Kraft studied electrical engineering at the University of Applied Science in Hanover and renewable energies at the University of Applied Science in Berlin. He received his master's degree in renewable energies before joining Fraunhofer ISE as a Ph.D. student in 2012. In 2015 he received his Ph.D. in the field of plated-copper front-side metallization for silicon solar cells. Since then he has focused on solar cell interconnection technologies and processes as head of the interconnection technologies team at Fraunhofer ISE.

Dr. Ulrich Eitner studied technical mathematics at the University of Karlsruhe (TH) and received his Diploma degree in 2006 for his development of a simulation method for multibody dynamics. From 2006 to 2011 he worked in the field of PV modules at the Institute for Solar Energy Research Hamelin (ISFH), and obtained his Ph.D. from the University of Halle-Wittenberg in 2011 for his investigations of the thermomechanics of PV modules. In 2011 he joined Fraunhofer ISE in Freiburg as head of the PV modules group, focusing on interconnection technology for crystalline silicon solar cells, analysis of cell-to-module efficiencies, and novel module concepts.

Enquiries

Angela De Rose
Team Interconnection Technology
Division Photovoltaics
Fraunhofer Institute for Solar Energy Systems ISE
Heidenhofstraße 2
79110 Freiburg, Germany

Tel: +49 (0)761 4588 5856
Email: angela.de.rose@ise.fraunhofer.de